Pitch Motion Control without Braking Distance Extension considering Load Transfer for Electric Vehicles with In-Wheel Motors

Ting Qu*, Hiroshi Fujimoto, Yoichi Hori (The University of Tokyo)

Abstract: Pitch motion occurs due to load transfer during vehicle deceleration or acceleration. By utilizing In-Wheel motors, load will be transferred not only based on vehicle dynamics, but also depend on anti-dive/lift force. Also, the anti-dive/lift force is influenced by driving/braking force. Thus, by considering driving/braking force distribution on front and rear wheels, pitch motion can be suppressed without braking distance extension. In this paper, the vehicle dynamic modeling is presented including modeling parameter identification. Then the controller design is explained. Also simulations and experiments are carried out to verify this proposed control system. Finally, the conclusion is presented.

Keywords: Pitch motion, braking distance, load transfer, anti-dive/lift force, driving/braking force

1. Introduction

With the big problem of global warming, more and more research groups have been studying on electric vehicles (EVs). Since electric motors and inverters are utilized in drive system, they have great advantages over internal combustion engine vehicles (ICEVs). The advantages of EVs are summarized as [(1)],

1. Quick torque response
   The electric motor's torque response is 100-500 times as fast as ICEVs;
2. Motor torque can be measured easily
   In ICEVs, it is difficult to accurately measure the output torque. On the other hand, the output torque of electric motor can be measured easily from current. Therefore, the state of the road can be estimated;
3. Individual wheel control
   By using in-wheel motors, each wheel can be independently driven. Then, individual wheel control can enhance the vehicle stability;

The research fields of motion control of EVs are classified as driving safety (Traction control [(2)], Direct-yaw control [(3)] and Anti-slip control [(4)]), driving comfort (Roll [(5)], Pitch control) and economy (Range Extension Control [(6)]). Especially, in this paper, from the viewpoint of driving comfort research field, the author focus on pitch motion control without braking distance extension. Pitch motion occurs when vehicle accelerating, decelerating or passing barriers. Especially, when vehicle is decelerating, due to the inertia force, vehicle body could turn to nose-dive and tail-lift. This motion has negative influence of driving comfort, thus it should be considered.

Currently, the active suspension design [(7)] and control [(8)] are the current comparatively effective ways to improve driving comfort and are being engineered in partial exclusive vehicles. However, because of the high cost, it is difficult to be widespread in common vehicles. On another hand, since In-Wheel Motor is installed below suspension, there is a force of vertical direction generated during vehicle driving. This force is named anti-dive/lift force [(9)]. Moreover, the magnitude of anti-dive/lift force depends on driving/braking force. Therefore, by controlling driving/braking force, the anti-dive/lift force can be utilized for pitch motion control. Based on this idea, the conventional pitch motion control based on method of 2DOF has been proposed [(10)]. However, in this case, the only In-Wheel Motors on the rear wheels are used. This means, there is only one DOF on the longitudinal direction. Thus though pitch motion is controlled, the braking distance is extended.

Based on this problem, a novel pitch motion without braking distance extension considering load transfer is proposed. An EV in which 4 wheels are attached with In-Wheel Motors is utilized. By considering the distribution of driving/braking forces of front and rear wheels, it is feasible to generate anti-dive/lift force to balance load transfer without braking distance extension.

The remainder of this paper is organized as follows: Section 2 states the proposed vehicle dynamics modeling; section 3 explains the controller design; section 4 shows the simulation results while section 5 shows the experiment results; section 6 is the conclusion.

2. Vehicle Dynamics

2.1 Vehicle Modeling

The rotational dynamics equation of front/rear two wheels is given as

$$T_{mi} + T_{rb} - r \cdot F_{di} = 2J_{\omega i} \cdot \dot{\omega}_i \,. \tag{1}$$

Here, T_{mi} is motor torque generated from proposed controller; T_{rb} is regenerative braking torque; $T_i = T_{mi} + T_{rb}$ is total motor torque as the input into vehicle plant; r is radius of wheel; F_{di} is driving/braking force; $J_{\omega i}$ is wheel inertia; ω is angular velocity of wheel. Since the longitudinal direction of vehicle dynamics is considered, the left and the right sides of vehicle are symmetrical. The subscript i stands for front two wheels f and rear two wheels r.

The motion equation of vehicle on longitudinal direction is described as

$$m \cdot \dot{V} = m \cdot a_x = F_d - F_{dr} \,. \tag{2}$$

Here, m is vehicle mass; V is vehicle velocity; a_x is acceleration; F_d is total driving/braking force. Here, the driving resistance F_{dr} is ignored.

Also the relationship between driving/braking and friction coefficient is expressed as

$$F_{di} = F_{zi} \cdot \mu(\lambda_i) \,. \tag{3}$$

Here, F_{zi} is load on vertical direction; μ is friction coefficient; λ is slip ratio whose equation is shown as

$$\lambda_i = \frac{V_{\omega i} - V}{\max(V_{\omega i}, V, \varepsilon)} \,. \tag{4}$$

Here, $V_{\omega i}$ is wheel velocity; ε is a small constant value avoiding λ becoming 0. Based on Eq. (1) ~ (4), the block vehicle dynamics modeling which is applied for simulation is shown in Fig.1.

In this paper, Magic Formula is adopted as the simulation model between the friction coefficient μ and the slip ratio λ [(11)].

2.2 Pitch Motion Modeling

Since vehicle dynamics is bilateral symmetry, the half vehicle dynamics model is designed and shown in Fig.2. Because pitch motion is a rotational motion around center of Gravity (CoG) and causes vehicle body attitude change, the vehicle body can be approximated to the model of rigid body. Moreover, tire can be simplified as a combination of damper and spring.

From Fig.2, the transfer function between pitch angle θ and pitch moment M is expressed as

$$\frac{\theta}{M} = \frac{1}{Is^2 + Cs + K} \,, \tag{5}$$

where pitch moment is expressed as

$$M = F_{zf} \cdot l_f - F_{zr} \cdot l_r \,. \tag{6}$$

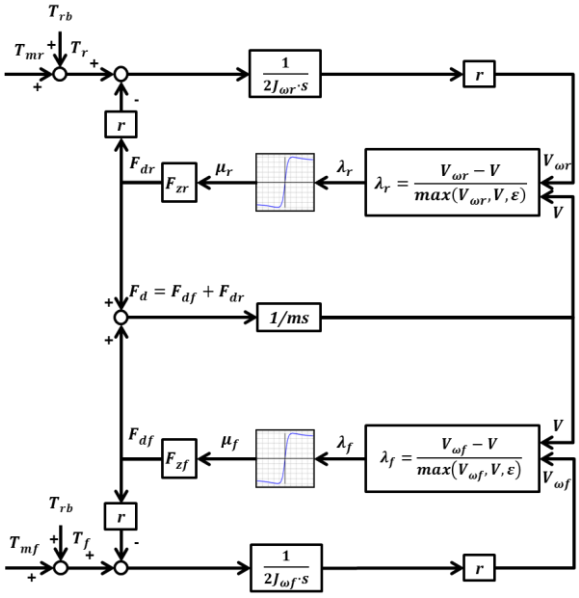

Fig.1 Block diagram of vehicle modeling

Here, I is inertia moment around y axis; C is damping coefficient; K is spring constant; h is height from ground to CoG; l_i is distance from CoG to wheelbase.

In Eq. (6), equations of loads of front and rear wheels are expressed as

$$F_{zf} = F_{zof} - a_x \cdot m \cdot \frac{h}{l_f + l_r} + F_{df} \cdot \tan\varphi_f \tag{7}$$

$$F_{zr} = F_{zor} + a_x \cdot m \cdot \frac{h}{l_f + l_r} - F_{dr} \cdot \tan\varphi_r \,. \tag{8}$$

Here, F_{zoi} is static load; φ_i is angle between horizontal line and linked line from tire road contact point to point of Instantaneous Centers of Rotation (ICR) whose geometry structure is shown in Fig.3.

On the right side of Eq. (7) and (8), the first term is vehicle static load; the second term is load transfer caused by vehicle

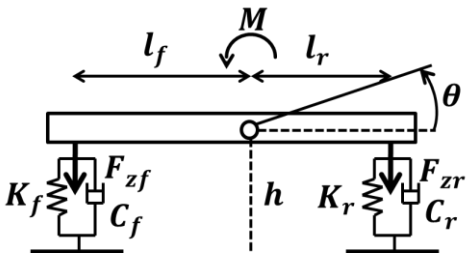

Fig.2 Half vehicle model

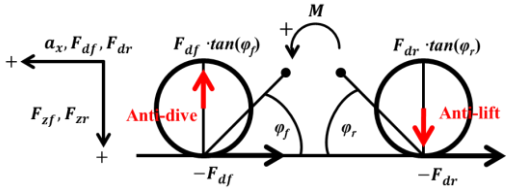

Fig.3 Geometry of anti-dive/lift force

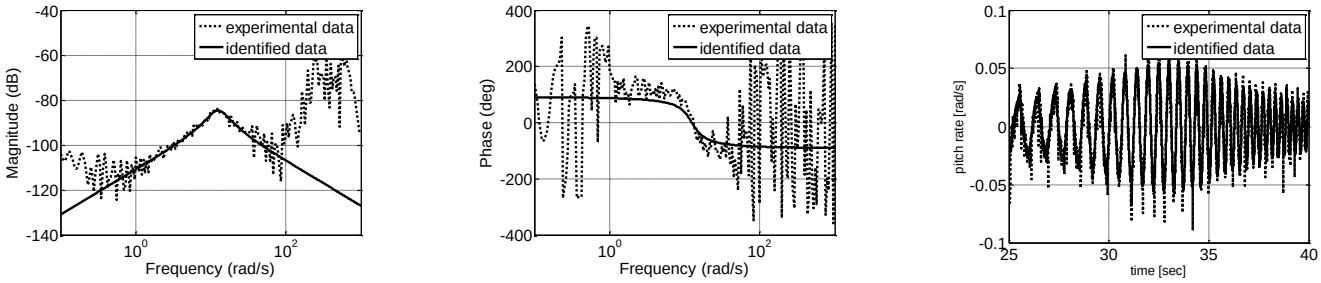

(a) Magnitude of bode diagram (b) Phase of bode diagram (c) Pitch rate

Fig.4 Parameters identification of front wheels

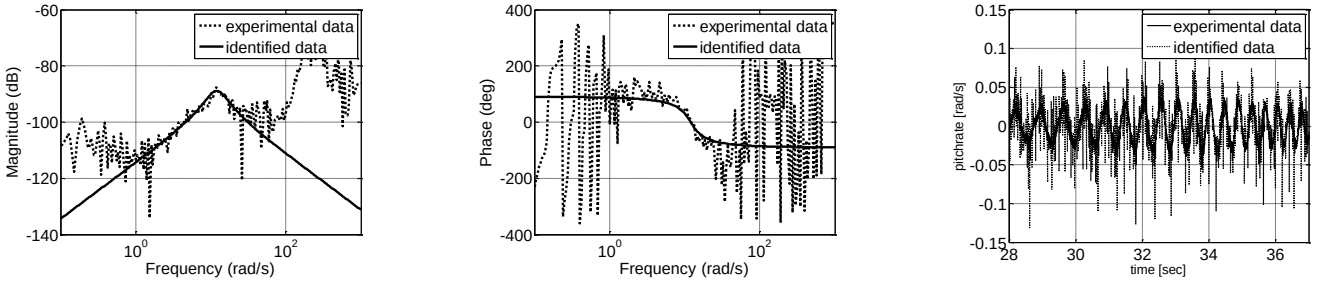

(a) Magnitude of bode diagram (b) Phase of bode diagram (c) Pitch rate

Fig.5 Parameters identification of rear wheels

dynamics; the third term is anti-dive/lift force. Fig.3 shows the geometry structure of generation of anti-dive/lift force. When vehicle decelerates, the driving/braking force F_{di} acts on tire road contact point due to mechanical structure of In-Wheel Motor [12], and this force can be transferred to suspension through brake units. As a result, anti-dive force on front wheels can be expressed by $F_{df} \cdot \tan\varphi_f$, while anti-lift force on rear wheels can be expressed by $F_{dr} \cdot \tan\varphi_r$.

Then, by substitute (7) and (8) into (6), and then by substitute (6) into (5), the final transfer function is expressed as

$$\theta = \frac{G_1}{Is^2 + Cs + K} F_{df} + \frac{G_2}{Is^2 + Cs + K} F_{dr}, \tag{9}$$

which is assumed the static moment $F_{zof} \cdot l_f - F_{zor} \cdot l_r = 0$. G_1 and G_2 are derived as

$$G_1 = -h + \tan\varphi_f \cdot l_f \tag{10}$$

$$G_2 = -h + \tan\varphi_r \cdot l_r . \tag{11}$$

2.3 Parameter Identification of Pitch Model

The experiment for unknown parameters identification is carried out. First, the sine sweep motor torque T_{mi} is given as the input into front and rear two wheels, respectively. The output of pitch rate is measured from gyro sensor. Second, by using method of FFT, unknown parameters are identified. Experimental results are shown in Fig.4 and 5. The transfer function is expressed as

$$\dot{\theta} = \frac{-0.28s}{616s^2 + 4683s + 88704} F_{df} + \frac{-0.17s}{616s^2 + 4683s + 88704} F_{dr} . \tag{12}$$

Here, inertia moment is calculated by $I = m \cdot l_f \cdot l_r$; natural angular frequency $\omega_n = 12$[rad/s]; damping constant $\zeta = 0.3$; angle $\varphi_f = 10.4^\circ$; $\varphi_r = 22.5^\circ$.

3. Controller Design

The control objective is to suppress pitch motion and improve driving comfort without braking distance extension. As equations defined in (7) and (8), the magnitude changing of load is influenced by anti-dive/lift force. In addition, anti-dive/lift force is related with driving/braking force F_{di} and φ_i. φ_i has been determined already from experiment of parameters identification. Therefore, load transfer is controlled by driving/braking force F_{di}. Based on this idea, a novel pitch motion control without braking distance extension considering load transfer is proposed.

The block diagram of controller is shown in Fig.6 in which there are two independent control loops: one is pitch motion control loop; the other is deceleration control loop.

3.1 Pitch Motion Control

Pitch motion control is designed based on Eq. (5).

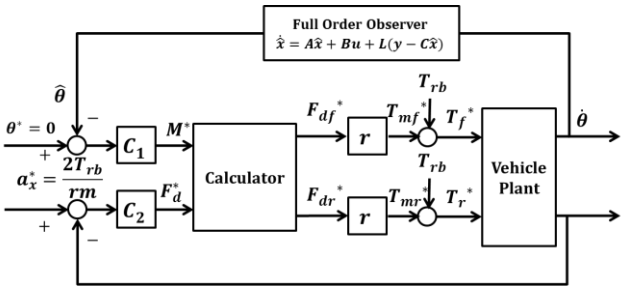

Fig.6 Block diagram of control of pitch motion without braking distance extension considering load transfer

Note that the pitch angle θ cannot be measured directly due to sensor cost problems. Therefore we have proposed the state observer for pitch angle estimation. The state space equation is given as

$$\dot{x} = Ax + Bu \tag{13}$$

$$y = Cx, \tag{14}$$

where

$$A = \begin{bmatrix} 0 & 1 \\ -\frac{K}{I} & -\frac{C}{I} \end{bmatrix}, B = \begin{bmatrix} 0 & 0 \\ \frac{G_1}{I} & \frac{G_1}{I} \end{bmatrix}, C = \begin{bmatrix} 1 & 0 \end{bmatrix}, x = \begin{bmatrix} \theta \\ \dot{\theta} \end{bmatrix}, u = \begin{bmatrix} F_{df} \\ F_{dr} \end{bmatrix}. \tag{15}$$

From Eq. (15), the state variables are pitch angle and rate while the control inputs are driving/force of front and rear wheels. The observer gain K_{gain} is designed as

$$K_{gain} = \begin{bmatrix} -(r_1 + r_2) - \frac{C}{I} \\ r_1 \cdot r_2 - \frac{K}{I} \end{bmatrix}, \tag{16}$$

where r_1 and r_2 are the poles of observer.

The reference of pitch angle is given as $\theta^* = 0$. PD controller C_1 is designed based on pole placement method to generate the reference pitch moment M^*.

3.2 Deceleration Control

Deceleration control is designed based on Eq. (2). The reference of deceleration a_x^* is calculated by

$$a_x^* = \frac{2 \cdot T_{rb}}{m \cdot r}, \tag{17}$$

where T_{rb} is the driver command of regenerative braking torque. Moreover, in deceleration control loop, PI controller C_2 is designed based on pole placement method to generate the reference of total driving/braking force F_d^*. From controller C_1 and C_2, the references of pitch moment M^* and total driving/braking force F_d^* are generated. Then through driving/braking force distribution calculator, the references of driving/braking force on front and rear wheels F_{df}^* and F_{dr}^* are produced. The matrix of driving/braking force distribution calculator is expressed as

$$\begin{bmatrix} F_{df}^* \\ F_{dr}^* \end{bmatrix} = \frac{1}{\tan\varphi_r \cdot l_r - \tan\varphi_f \cdot l_f} \begin{bmatrix} -h + \tan\varphi_r \cdot l_r & -1 \\ -(-h + \tan\varphi_f \cdot l_f) & 1 \end{bmatrix} \begin{bmatrix} F_d^* \\ M^* \end{bmatrix}. \tag{18}$$

4. Simulation

The simulation conditions are given as follows: first, assuming, vehicle is running on the high $\mu(\mu = 0.9)$ road at an initial vehicle velocity V_0=3.5[m/s]; then vehicle starts to decelerate at 1sec by giving the regenerative brake torque $T_{rb} = -80$[Nm] on front and rear two wheels. At the same time (1sec), controller begins to work. Some parameters are used as: $J_{\omega f}$ =1.24[Nm^2]; $J_{\omega r}$ = 1.26[Nm^2], $r = 0.302$[m], l_f =0.999[m], l_r =0.701[m] and m = 850[kg].

The simulation results are shown in Fig.7. The poles of controller C_1 and C_2 are set at -15[rad/s] and -5[rad/s]. Fig.7 (a) and (b) are the simulation results of pitch angle $\hat{\theta}$ and pitch rate $\dot{\theta}$. Both pitch angle and rate are suppressed. Especially, from Fig.7 (a), pitch angle is reduced by 30% while from Fig.7 (b), pitch rate is also reduced to improve the driving comfort. Fig.7 (c) shows the braking distance. Since deceleration control is applied, the braking distance is shortened about 0.8m. Fig.7 (d) is simulation result of deceleration control loop. The feedback signal of deceleration is well followed with reference value. Fig.7 (e) is the motor toque T_i. There is a driving/braking torque distribution of front and rear wheels. Especially, the motor torque on rear wheels is generated much more. Fig.7 (f) shows the anti-lift force. Because the much more motor torque on rear wheels is generated, the much more anti-lift force on rear wheels is produced and this force has the possibility to balance pitch motion. Fig.7 (g) shows reference of pitch motion M^* that generated from pitch motion control loop while Fig.7 (h) shows the reference of driving/braking force F_d^* that produced from deceleration control loop.

5. Experiment

5.1 Experimental Vehicle

The characteristic of the experimental EV “FPEV2-Kanon” are introduced. “FPEV2-Kanon” is utilized for implementing various motion controls, in which, the outer rotor type In-Wheel Motors are attached on each wheel. Also, since these motors can be driven directly, it is possible to transfer the reaction force from road side to motor side without considering the influence of backlash from reduction gears. Each motor can be independent driven. Besides, the maximum torques of front and rear motors are ± 500 [Nm] and ± 340 [Nm] respectively. Fig.8 (a) shows picture of FPEV2-Kanon; (b) shows In-Wheel Motor on the rear wheel of left side; Table 1 shows specification of experimental EV.

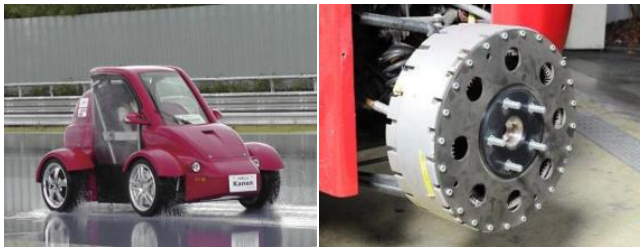

(a) FPEV2-Kanon (b) In-Wheel Motor

Fig.8 Experimental EV

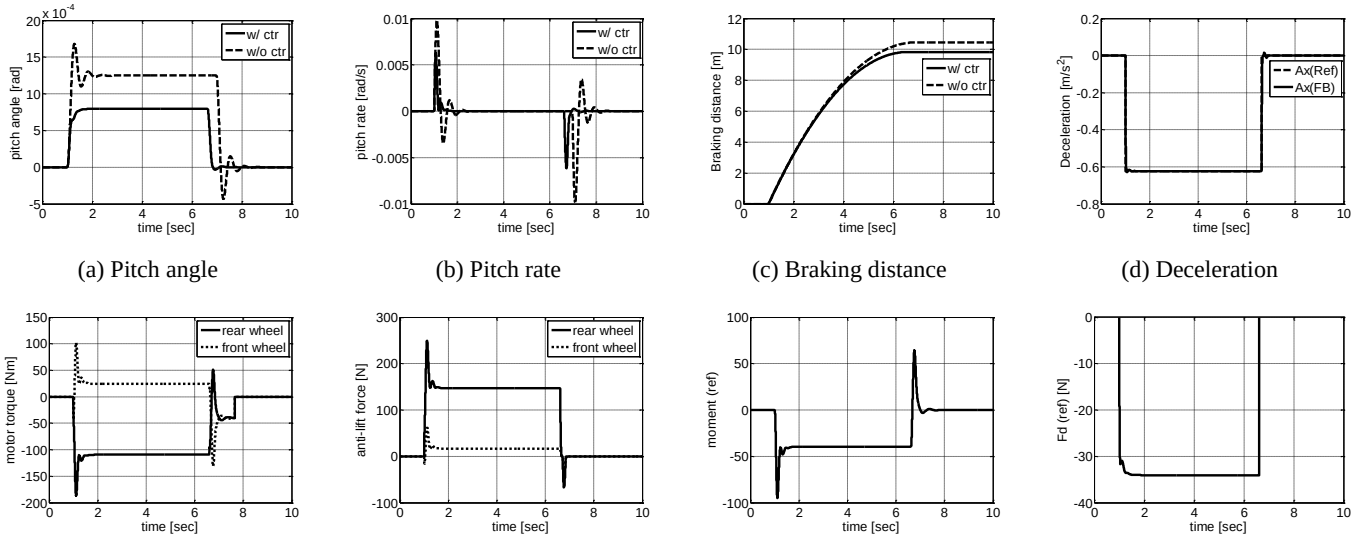

(a) Pitch angle (b) Pitch rate (c) Braking distance (d) Deceleration

(e) Motor torque T_i (f) Anti-lift force (anti-lift force of front wheels: $F_{df} \cdot \tan\varphi_f$ Anti-lift force of rear wheels: $-F_{dr} \cdot \tan\varphi_r$) (g) Reference of pitch moment M^* (h) Reference of driving/braking force F_d^*

Fig.7 Simulation results

Table 1 Specification

Dimensions (L×W×H)	2300×1600×1510 mm
Weight	850 kg
Vehicle Inertia	616 kgm^2
l_f	999 mm
l_r	701 mm
Tread Base	1300 mm
Radius of Tire	302 mm

5.2 Experiment Results

The experimental results are shown in Fig.9. The experiment condition is assumed as: vehicle is running on high $\mu(\mu = 0.9)$ road at a constant velocity of 14.4km/h. From 1sec, vehicle begins to decelerate by giving regenerative braking torque command of T_{rb}=-80[Nm] on front and rear two wheels. Also, at the same time (1sec), controller begins to work.

Moreover, pole of observer is set at -3[rad/s]; pole of PD controller of pitch motion is set at -15[rad/s]; pole of PI controller of deceleration is set at -2[rad/s].

Fig.9 (a) and (b) show the experimental results of pitch angle and the pitch rate. Both pitch angle and rate are suppressed compared with the case of without control. In particular, pitch angle is reduced by 25% and driving comfort is improved. Fig.9 (c) shows the experimental result of braking distance. Since deceleration control is applied, the braking distance is shortened by 0.3m. Fig.9 (d) shows experimental result of deceleration control loop. In this paper, the feedback deceleration signal is used by a differential of vehicle velocity and vehicle velocity is measured by the optical sensor. If the optical sensor is not setup, it is still can be realized through method without vehicle velocity detection [13]. From the start time of 1sec, the feedback signal of deceleration is going to follow the reference value gradually. However, from 3sec, the feedback signal of deceleration is over the reference value slightly. This leads that there is a change of direction of motor torque whose result is shown in Fig.9 (e). Fig.9 (e) shows the measured motor torque T_i of front wheels and rear wheels. First, a distribution of motor torque between front wheels and rear wheels is exist due to driving/braking force distribution calculator. Especially, there are much more torque on the rear wheels is generated. However, due to the negative influence of deceleration control, second, a change of direction of motor torque T_i can be found. Fig.9 (f) shows the reference pitch moment generated from pitch motion control loop.

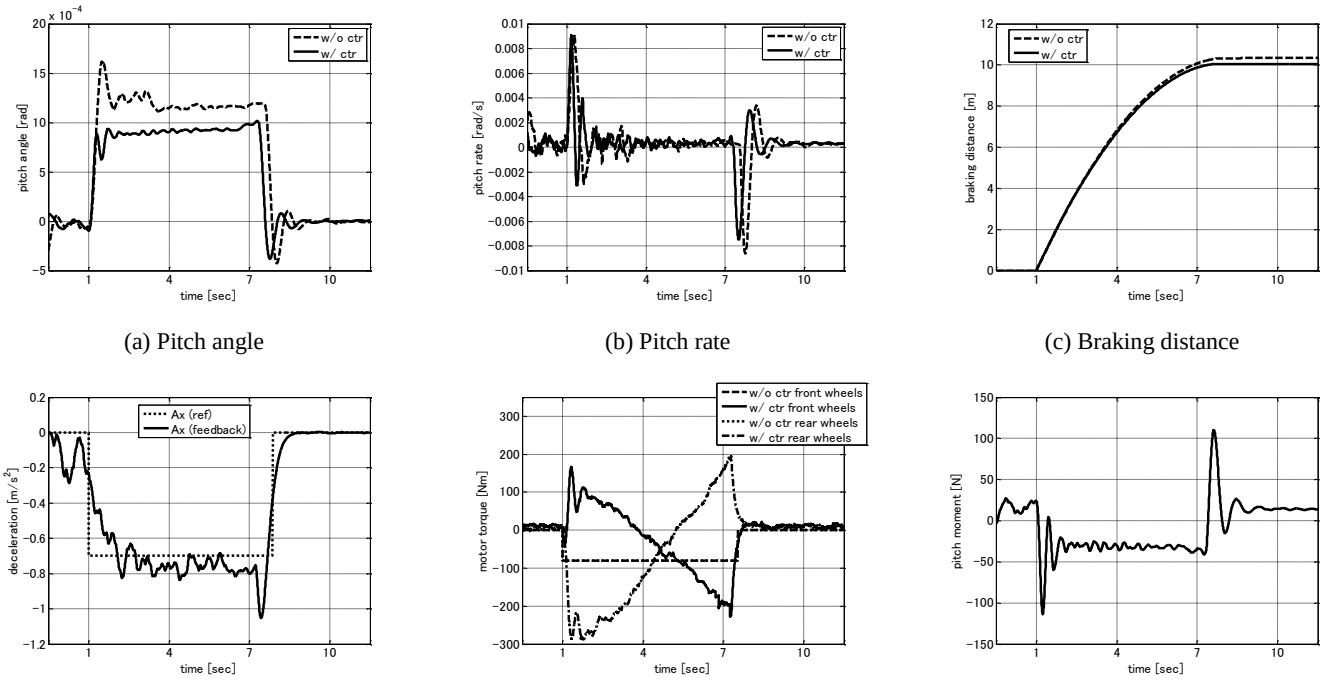

(a) Pitch angle　(b) Pitch rate　(c) Braking distance

(d) Deceleration　(e) Measured motor torque T_i　(f) Reference of pitch moment M^*

Fig.9 Experimental results

6. Conclusion

In this paper, from the view point of vehicle driving comfort, the research on pitch motion control without braking distance extension considering load transfer is studied. Since a vertical force of anti-dive/lift is produced based on driving/braking force, it is possible to change loads on front and rear wheels and balance pitch motion. Therefore, authors have proposed a novel pitch motion control without braking distance extension considering load transfer with In-Wheel Motors. Moreover, the proposed control method is verified both through simulation and experimental results.

Acknowledgement

This research was partly supported by the Industrial Technology Research Grant Program from the New Energy and Industrial Technology Development Organization (NEDO) of Japan and in part by the Ministry of Education, Culture, Sports, Science and Technology grant number 22246057.

References

(1) Y. Hori, Future Vehicle driven by Electricity and Control-Research on Four Wheel Motored UOT Electric March II, IEEE Transaction on Industrial Electronics, Vol.51, No.5, October 2004.

(2) D. Yin, Y. Hori, A new approach to traction control of EV based on maximum effective torque estimation, IECON, pp.2764 – 2769, 2008.

(3) F. Li, Fuzzy-Logic-Based Controller Design for Four-wheel-drive Electric Vehicle Yaw Stability Enhancement, FSKD, 2009.

(4) M. Jalili-Kharaajoo, Sliding mode traction control of an electric vehicle with four separate wheel-drives, ETFA, 291 - 296 vol.2, 2003.

(5) K. Kawashima, Y. Hori, Rolling Stability Control of In-wheel Electric Vehicle Based on Two Degree of Freedom Control, Advanced Motion Control, pp.751-756, 2008.

(6) H. Sumiya, H. Fujimoto, Range Extension Control System for Electric Vehicle with Active Front Steering and Driving/Braking Force Distribution on Curving Road, in Proc. 36th Annual Conference of the IEEE Industrial Electronics Society, pp.2346-2351, 2010.

(7) J. Cao, An improved Active Suspension Model for Attitude Control of Electric Vehicles, Mechatronics and Automation, pp.147-152, 2007.

(8) S. Abu Bakar, Ride Comfort Evaluations on Electric Vehicle Conversion and Improvement Using Magnetorheological Semi Active Suspension System, SICE, pp.305-311, 2011.

(9) E. Katsuyama, Decoupled 3D Moment Control by In-Wheel Motor, Society of Automotive Engineers of Japan, No.3-11, pp.1-6, 2011.

(10) S. Sato, H. Fujimoto, Proposal of Pitching Control Method Based on Slip-Ratio Control for Electric Vehicle, IECON, pp.2823-2828, 2008.

(11) H. B.Pacejka, E.Bakker: "The magic formula tyre model", Tyre models for vehicle dynamic analysis: proceedings of the 1st International Colloquium on Tyre Models for Vehicle Dynamics Analysis, held in Delft, The Netherlands (1991)

(12) Vehicle Motion Performance and Chassis Mechanism

(13) T. Suzuki, H. Fujimoto, "Slip Ratio Estimation and Regenerative Brake Control without Detection of Vehicle Velocity and Acceleration for Electric Vehicle at Urgent Brake-turning", in Proc., Niigata, pp. 273-278, 2010.